Effects of Ekman Transport on the NAO Response to a Tropical Atlantic SST Anomaly

SHILING PENG

NOAA–CIRES Climate Diagnostics Center, University of Colorado, Boulder, Colorado

WALTER A. ROBINSON

Department of Atmospheric Sciences, University of Illinois at Urbana–Champaign, Urbana, Illinois

SHUANGLIN LI AND MICHAEL A. ALEXANDER

NOAA–CIRES Climate Diagnostics Center, University of Colorado, Boulder, Colorado

(Manuscript received 15 July 2005, in final form 7 February 2006)

ABSTRACT

A recent study showed that a tropical Atlantic sea surface temperature (SST) anomaly induces a significant coupled response in late winter [February–April (FMA)] in a coupled model, in which an atmospheric general circulation model is coupled to a slab mixed layer ocean model (AGCM_ML). The coupled response comprises a dipole in the geopotential height, like the North Atlantic Oscillation (NAO), and a North Atlantic tripole in the SST. The simulated NAO response developed 1 or 2 months later in the model than in observations. To determine the possible effects of Ekman heat transport on the development of the coupled response to the tropical forcing, an extended coupled model (AGCM_EML), including Ekman transport in the slab mixed layer ocean, is now used. Large ensembles of AGCM_EML experiments are performed, parallel to the previous AGCM_ML experiments, with the model forced by the same tropical Atlantic SST anomaly over the boreal winter months (September–April).

The inclusion of Ekman heat transport is found to result in an earlier development of the coupled NAO–SST tripole response in the AGCM_EML, compared to that in the AGCM_ML. The mutual reinforcement between the anomalous Ekman transport and the surface heat flux causes the tropical forcing to induce an extratropical SST response in November–January (NDJ) in the AGCM_EML that is twice as strong as that in the AGCM_ML. The feedback of this stronger extratropical SST response on the atmosphere in turn drives the development of the NAO response in NDJ. In FMA, the sign of the anomalous surface heat flux is reversed in the Gulf Stream region such that it opposes the anomalous Ekman transport. The resulting equilibrium NAO response in the AGCM_EML is similar to that in the AGCM_ML, but it is reached 1–2 months sooner in the AGCM_EML. Hence, the presence of Ekman transport causes a seasonal shift in the evolution of the coupled response. The faster development of the NAO response in the AGCM_EML suggests that tropical Atlantic SST anomalies should be able to influence the NAO, in nature, on the seasonal time scale, and that efficient interactions with the extratropical ocean play a significant role in determining the coupled response.

1. Introduction

Atmospheric variability over the North Atlantic in boreal winter is dominated by the North Atlantic Oscillation (NAO), which is characterized by a north–south pressure dipole centered near Iceland and Azores (see the review by Marshall et al. 2001). NAO variability is believed to be driven primarily by processes internal to the atmosphere, since both the structure and the variance of the NAO are largely simulated in atmospheric general circulation models (AGCMs) with climatological boundary conditions. To this extent, the NAO is inherently unpredictable beyond the short time scale, on the order of a few days, of intrinsic atmospheric predictability. Several recent studies, however, suggest that the NAO can be induced by forcing external to the atmosphere, such as SST anomalies (e.g., Rodwell et al. 1999; Watanabe and Kimoto 2000; Sutton et al. 2001; Peng et al. 2002, 2003; Drevillon et al. 2003). Since SST anomalies often persist for months

Corresponding author address: Dr. Shiling Peng, NOAA–CIRES CDC, R/PSD1, 325 Broadway, Boulder, CO 80305-3328. E-mail: Shiling.Peng@noaa.gov

and possess significant variance on interannual-to-decadal time scales (e.g., Deser and Blackmon 1993; Kushnir 1994; Wu and Liu 2005), their influences on the NAO, if properly identified, may provide some predictability for the NAO at these low frequencies.

One pattern of SST anomalies that has been identified in recent GCM studies to be effective in forcing the NAO is the SST tripole in the North Atlantic, related to the NAO by simultaneous linear regression (e.g., Rodwell et al. 1999; Sutton et al. 2001; Peng et al. 2002, 2003). While the tripole may initially be forced by the NAO, these studies reveal that it can also induce a reinforcing NAO-like response. This suggests that, in nature, the NAO and the tripole may act to reinforce and maintain each other in producing enhanced and persistent coupled variability. Apart from GCM studies, Czaja and Frankignoul (2002, hereafter CF02) sought to identify SST influences on the NAO in observations, through a lead–lag maximum covariance analysis (MCA) of the observed 500-hPa geopotential height (Z500) over the Atlantic and Atlantic SST anomalies north of 20°S. Their MCA results revealed that a fall Pan-Atlantic SST anomaly, composed of a horseshoe-like dipole in the North Atlantic and a southern center in the equatorial Atlantic, tends to precede the winter NAO by a few months. Further calculations, using only the extratropical or only the tropical SST, yielded similar results. It was thus suggested that the winter NAO can be influenced by both the North Atlantic horseshoe (NAH) and the tropical anomaly that persist from the fall into the winter.

To determine if these lagged relationships between the fall SST anomalies and the winter NAO may indeed arise from the SST forcing of the NAO, Peng et al. (2005) conducted large ensembles of model experiments examining the atmospheric responses to the NAH and to the tropical SST anomaly, along other efforts on the problem (e.g., Drevillon et al. 2003; Rodwell et al. 2004; Cassou et al. 2004). Two models were used: an AGCM and a coupled model, AGCM_ML, in which the AGCM was coupled to a slab mixed layer ocean. The AGCM results demonstrate that the NAH anomaly induces a baroclinic atmospheric response throughout boreal winter that projects little on the NAO. Hence, unlike the SST tripole, which, in the same AGCM, induces an eddy-forced NAO-like response (Peng et al. 2002, 2003), the NAH anomaly is found ineffective in perturbing the storm tracks to generate such a response. A similar baroclinic response to a NAH-like anomaly in boreal winter is also evident in the multimodel ensemble mean shown in Rodwell et al. (2004, their Fig. 2). This suggests that the observed relationship between the fall NAH SST and the winter NAO is unlikely to result from the NAH SST forcing the NAO.

The tropical anomaly in the AGCM_ML, in contrast, induces a strongly seasonal coupled response in the North Atlantic, with the NAO and SST tripole appearing late in the winter [February–April (FMA)], through "the atmospheric bridge" as in the Pacific (e.g., Lau and Nath 1996; Alexander et al. 2002). In early winter [October–December (OND)], anomalous atmospheric geopotential heights are characterized by a wave train propagating to the northeast, accompanied by a NAH-like SST response. The AGCM_ML results, therefore, suggest that the observed lagged relationship between the NAH SST and the NAO (or the SST tripole) may arise from the seasonal march of the coupled response to a persistent remote forcing, such as the tropical Atlantic SST anomaly.

As pointed out in Peng et al. (2005), the tropical anomaly, however, should neither be considered as the solely possible, nor the most dominant, forcing of this coupled response. Persistent forcings in other oceanic basins, such as in the North Pacific (as indicated in Fig. 6 of CF02), could perhaps be more effective in inducing the Atlantic coupled response. This would readily explain why the lagged NAH SST–NAO relationship seems to also exist in nature independent of the tropical Atlantic anomalies (Frankignoul and Kestenare 2005). The model results described above, nevertheless, suggest that such a statistical relationship should neither be interpreted as necessarily indicating the NAH SST forcing of the NAO, nor the absence of its connections with the tropical Atlantic anomalies.

While the tropical SST-induced coupled response in the AGCM_ML agrees qualitatively with the observed lagged relationship of CF02, the NAO appears to develop earlier in nature [November–January (NDJ)] than in the model (FMA). This seasonal shift in the simulated NAO response may result from deficiencies in the AGCM or in the mixed layer model, but, considering that the mixed layer model takes into account only the effects of surface heat flux on the evolution of the SST, the latter is perhaps more likely. It has been suggested in previous studies (e.g., Frankignoul 1985; Seager et al. 2000, 2001) that, second to the surface heat flux, the most effective driver of SST variations is the wind-induced Ekman heat transport, especially along oceanic thermal fronts, such as the Gulf Stream in the North Atlantic and the Kuroshio Extension in the North Pacific. Because surface heat flux anomalies are, in general, proportional to anomalies in the air–sea temperature difference, for an equilibrium state with reduced air–sea temperature differences, anomalous Ekman transport may be expected to dominate the

anomalous surface heat flux, especially near ocean fronts (see also Haarsma et al. 2005).

Based on the anomalous wind stress associated with the tropical SST-forced NAO response in the AGCM_ML, it is estimated that, if included, Ekman heat transport may act to reinforce the anomalous surface heat flux to generate a stronger extratropical SST response. A more effective extratropical air–sea feedback may then affect the evolution of the coupled response to the tropical forcing. In this study, a new coupled model, AGCM_EML, is developed that includes Ekman transport in the slab mixed layer ocean. Experiments with the AGCM_EML, paralleling those conducted by Peng et al. (2005) with the AGCM_ML, reveal that the inclusion of Ekman transport indeed leads to a faster development of the NAO–tripole response to the tropical SST anomaly.

We present here the key results from the AGCM_EML experiments and compare them with the corresponding AGCM_ML results. The paper is organized as follows: section 2 describes the model experiments and the data analyses; section 3 presents model results in regard to intrinsic variability and the tropical SST-forced response; and a brief summary is given in section 4.

2. Methods

We briefly describe the model experiments and the data analyses used in the study. Many aspects of the methods are similar to those described in Peng et al. (2005), and so are not repeated in detail.

a. Model experiments

1) AGCM_EML EXPERIMENTS

The AGCM_EML is a coupled model with an AGCM coupled to a slab mixed layer ocean, in which the ocean temperature is determined by both the surface heat flux and the Ekman heat transport. The coupled domain is from 10°N to the climatological most advanced ice boundary over September–April, similar to that in the AGCM_ML of Peng et al. (2005). As described in Peng et al. (2002, 2003, 2005), the AGCM is a version of the seasonal forecast model used at the National Centers for Environmental Prediction (NCEP) in 2000. The model is configured with 28 levels and has a horizontal resolution corresponding to a T42 spectral truncation.

The slab mixed layer ocean, EML, is designed as an anomaly model with the mixed layer temperature (T) determined by only the (downward) surface heat flux (Q) and the linear horizontal advection by Ekman currents ($\mathbf{V}_E$) as follows:

$$\partial T'/\partial t = Q'/(\rho c_p h) - \mathbf{V}'_E \cdot \nabla \overline{T} - \overline{\mathbf{V}}_E \cdot \nabla T', \qquad (2.1)$$

where $\mathbf{V}_E = (\tau^x, -\tau^y)/(\rho f h)$, τ is the wind stress, h is the mixed layer depth (MLD), and the remaining symbols have their usual meanings. Overbars denote the daily climatology, and primes denote deviations from that climatology. The daily climatology for Q and τ is based on the smoothed ensemble mean of 60 AGCM control runs forced with the observed SST climatology. The mixed layer temperature anomaly, T', is calculated daily from Eq. (2.1), and then added to the observed SST climatology to drive the AGCM. The use of the anomaly model, as such, is equivalent to the use of the flux correction in Peng et al. (2005). It is implicit in this formulation that, with the SST at its climatological values, there is a balance among the climatological heat transports by Ekman currents, heat transports by the large-scale ocean circulation, and the exchanges of latent and sensible heat with the atmosphere.

To keep SST variance in the AGCM_EML similar to that in the AGCM_ML and in observations, the MLD in the AGCM_EML is set to 75 m, instead of 50 m as is used in the AGCM_ML. This adjustment is necessary because SST anomalies grow more rapidly in the AGCM_EML through the effects of Ekman transport. We choose to use a uniform MLD so that the model results are more compatible with those from the AGCM_ML, and that their differences are more readily interpreted. In a recent study by Ferreira and Frankignoul (2005), the observed MLD is used in their EML model and the resulting SST variability is underestimated by a factor of 2 in comparison with observations.

Following the AGCM_ML experiments conducted by Peng et al. (2005), a 100-member ensemble of 8-month (September–April) control runs is conducted with the AGCM_EML using the observed SST climatology south of 10°N. The ensemble is formed by initializing the runs with the NCEP reanalysis data of different dates from 1–5 September 1980 to 1999. In the coupled domain, the ensemble mean SST from the AGCM_EML control runs differs only slightly (~0.1 K) from the observed SST climatology averaged over September–April. Consistently, the ensemble mean atmospheric state of the AGCM_EML also differs little from that of the AGCM_ML and from that of the AGCM (Peng et al. 2002, 2005). To determine the coupled response to the tropical SST anomaly, two parallel 100-member ensembles of AGCM_EML runs are performed with the tropical anomaly added to or subtracted from the SST climatology. The model response is examined in this study as the ensemble-mean difference between the runs forced with the positive (P) and the negative (N) tropical anomaly. The statistical sig-

nificance of the response is estimated by a Student's *t* test, with each member of the ensemble taken as independent. All model results are based on twice-daily model outputs.

2) AGCM_ML AND AGCM EXPERIMENTS

The AGCM_EML results, in regard to both intrinsic variability and the SST-forced response, are compared with the corresponding results from the AGCM_ML runs of Peng et al. (2005). The AGCM_ML is similar to the AGCM_EML except that its slab ocean temperature is determined by the surface heat flux alone, and that the MLD is set to 50 m, as in some earlier studies (e.g., Lau and Nath 1996). The tropical SST-forced response from the parallel uncoupled AGCM runs of Peng et al. (2005) is also briefly compared.

b. Data analyses

1) EMPIRICAL ORTHOGONAL FUNCTION (EOF) ANALYSIS

To examine how the NAO is affected by the inclusion of Ekman transport in the AGCM_EML, in comparison with that in the AGCM_ML, an EOF analysis of the control run monthly Z500 in NDJ (and FMA) over the North Atlantic sector (20°–90°N, 90°W–90°E) is conducted for the two models, as in Peng et al. (2005). A corresponding analysis is also performed for the observed monthly Z500 of 1948–98, using the NCEP–National Center for Atmospheric Research (NCAR) reanalysis data.

2) MAXIMUM COVARIANCE ANALYSIS (MCA)

As in CF02, MCA is used to identify the dominant covarying patterns of Z500 and SST over the North Atlantic in the AGCM_EML and the AGCM_ML control runs. The analysis is performed for NDJ (and FMA) using monthly mean Z500 (15°–80°N, 100°W–20°E) and SST (15°–70°N, 80°W–0°) anomalies, normalized by a domain-averaged standard deviation, as in CF02, in order to give similar weight to each calendar month. We found, however, that the MCA results change little with or without this normalization.

3) TROPICAL SST ANOMALY

The tropical SST anomaly used in the AGCM_EML experiments is the same as that used in the AGCM_ML and the AGCM experiments of Peng et al. (2005). It is the tropical part (20°S–10°N) of the fall Pan-Atlantic SST pattern. This SST anomaly was identified by CF02, using a lagged MCA between the observed July–September (JAS) SST and NDJ Z500, as tending to lead the wintertime NAO. The details of how this anomaly is obtained are described by Peng et al. (2005).

4) SST VARIABILITY

Standard deviations, or root-mean-square (rms) variability, of monthly mean SST are calculated for the AGCM_EML and the AGCM_ML control runs, as well as for observations. The observed SST is based on the Global Sea Ice and Sea Surface Temperature (GISST) dataset for the period of 1946–99, as used in Peng et al. (2002).

3. Model results

a. Intrinsic variability

With a uniform MLD in the slab ocean model, we do not expect the simulated SST variability to match the observations in each month, as the seasonal cycle of the observed variability is also influenced by the varied MLD and other processes omitted in our simple models, such as the reemergence process (Alexander et al. 1999). The MLD defined in our models (75 m in the EML and 50 m in the ML) is mainly chosen to ensure that the simulated SST variability averaged over the period of the study is comparable to the observed. Figure 1 shows the monthly rms of SST anomalies averaged over October–April for the AGCM_EML and the AGCM_ML control runs and for observations. Overall, the SST variability in the two models captures the general features of the observed variability, with a center of action located in the western Atlantic near 45°N. Due to the effects of Ekman transport, the pattern of variability in the AGCM_EML more closely resembles the observed pattern than that in the AGCM_ML. In particular, its maximum occurs closer to the coast of Newfoundland. The amplitude of the averaged variability in the two models is comparable, with a maximum of about 1 K, which is only slightly stronger than observed (~0.8 K). In both models, the simulated variability thus constrained also matches well the observed in December (~1 K)—the center of the season (NDJ) focused on in this study (not shown). Given that the MLD is deeper in the AGCM_EML, it is evident from Fig. 1 that the Ekman heat transport contributes significantly to the growth of SST anomalies.

We have shown in Peng et al. (2005) that the effects of air–sea coupling on the atmospheric variability in the AGCM_ML, in both the total variance of monthly Z500 and its leading EOF, are modest. This is also

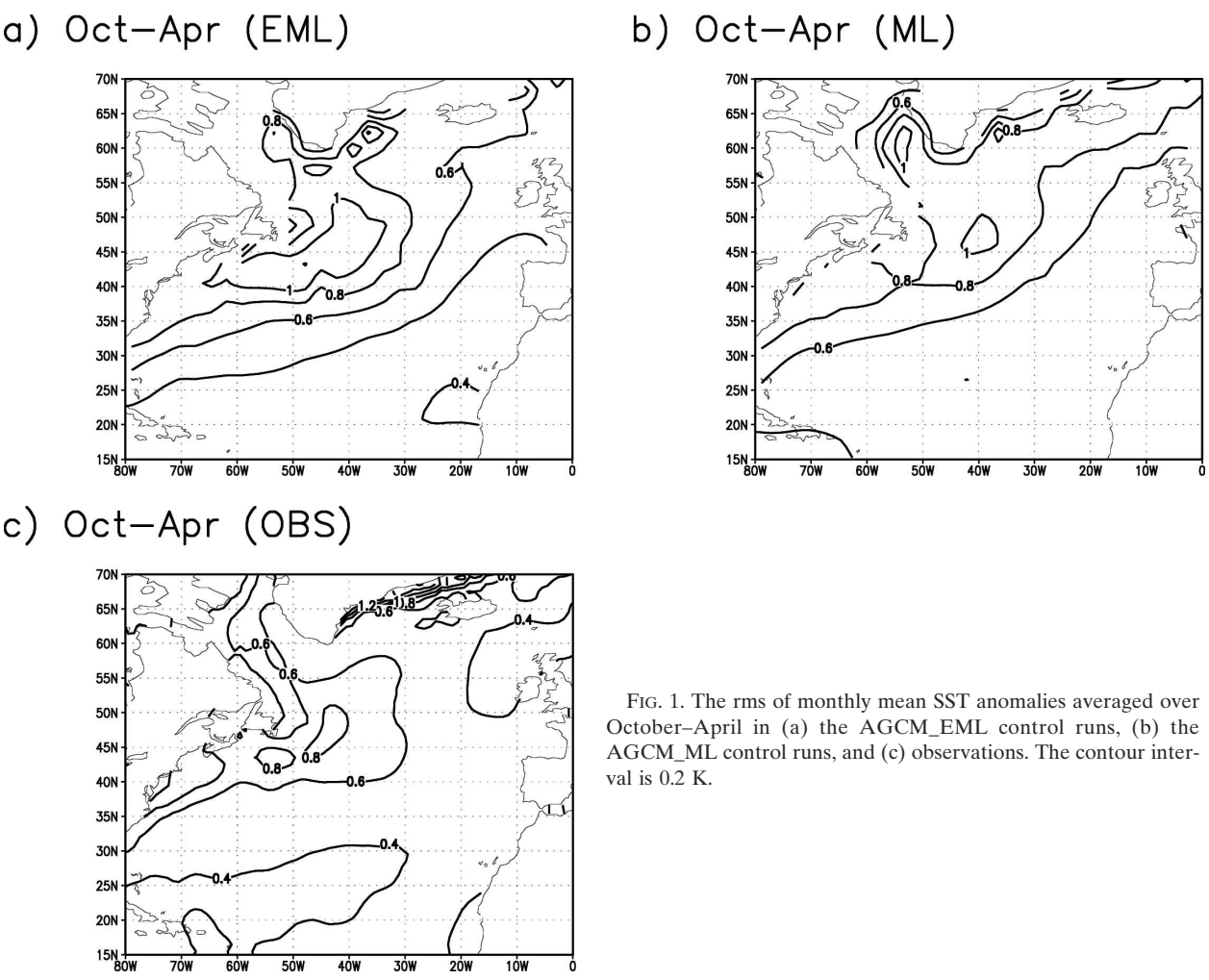

FIG. 1. The rms of monthly mean SST anomalies averaged over October–April in (a) the AGCM_EML control runs, (b) the AGCM_ML control runs, and (c) observations. The contour interval is 0.2 K.

largely the case in the AGCM_EML. As shown in Fig. 2 (left panels), the rms of monthly Z500 in NDJ in the two models is largely similar, and mostly captures the observed structure and amplitude. The simulated NAO variability, as represented by the leading EOF of monthly Z500, also resembles well the observed structure and the level of variance (Fig. 2, right panels). The inclusion of Ekman transport in the AGCM_EML results in some subtle differences in the NAO variability in NDJ (e.g., an enhanced southern center), in comparison with that in the AGCM_ML. The simulated variability in FMA in the two models is even more similar to each other (see Fig. 2 of Peng et al. 2005 for the AGCM_ML variability), and hence is not repeated here. The variance explained by the leading EOF in FMA is slightly increased in the AGCM_EML (by about 2%). The variance explained by the EOF2 is identical in the two models for both seasons.

To further determine the effects of Ekman transport on the coupled variability of the NAO–SST tripole, we compare the leading MCA mode of monthly mean Z500 and SST anomalies in NDJ (and FMA) in the AGCM_EML and the AGCM_ML control runs. The NDJ Z500 and SST covariance maps in both models (Fig. 3) exhibit a NAO-like Z500 dipole accompanied by a SST tripole, as in observations (CF02). The squared covariance explained by the leading mode, however, increases from 48% in the AGCM_ML to 53% in the AGCM_EML, which is closer to the observed value of 52% (see Fig. 5 of CF02). This variance increase appears to be robust, as we obtained similar results by reducing or increasing the spatial resolution of the model data in the MCA analysis. It is suggestive that the inclusion of Ekman transport enhances the coupled NAO–SST tripole variability in NDJ. In FMA, in contrast, the squared covariance explained by the leading MCA mode [featuring also the coupled NAO–tripole patterns (not shown)] is nearly the same in the

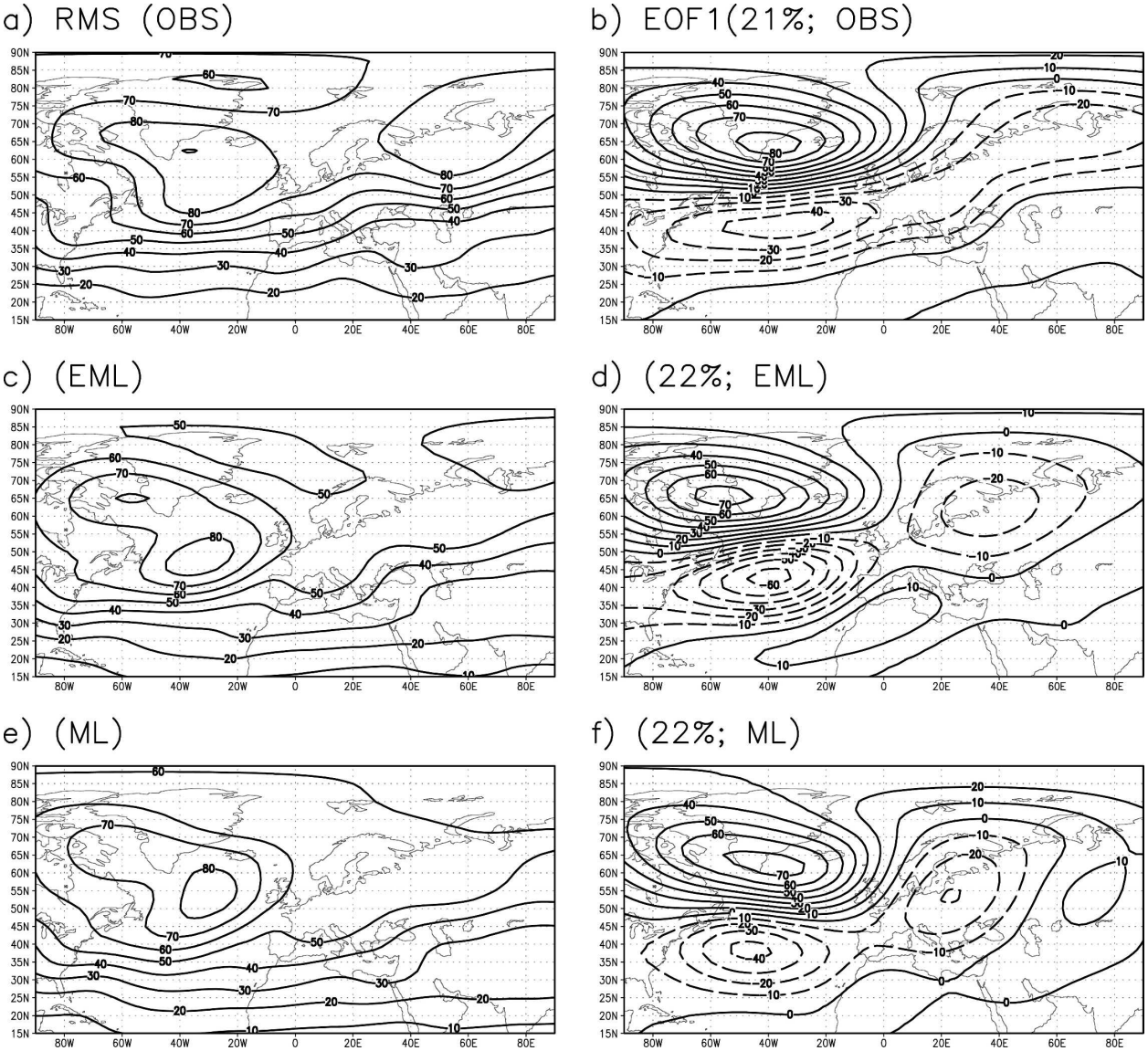

FIG. 2. The rms and the leading EOF of monthly Z500 in NDJ for (a), (b) observations; (c), (d) the AGCM_EML; and (e), (f) the AGCM_ML. The contour interval is 10 m. The percentage of the variance explained by the EOF is given in the brackets. In this and succeeding figures, dashed contours are used for negative values.

two models (62% and 61%). This seasonal difference in the influence of Ekman transport on the control-coupled variability is consistent with that on the tropically forced coupled responses, as discussed below.

b. Responses to the tropical SST anomaly

The tropical SST anomaly used to force the AGCM_EML, shown in Fig. 4, is centered in the equatorial eastern Atlantic, with a maximum strength of about 1.2 K. The Z500 response to the tropical anomaly in the AGCM_EML, as the (P − N) ensemble mean difference, is shown in Fig. 5 for October, NDJ, and FMA, along with the corresponding response in the AGCM_ML. Since the response is largely equivalent barotropic, the height anomalies at other levels are qualitatively similar to these at 500 mb. As discussed by Peng et al. (2005), in the AGCM_ML (Fig. 5, right panels), the Z500 response in early winter (October, NDJ) is dominated by a trough in the North Atlantic with a wave train to the northeast. In late winter (FMA) the response projects strongly on a negative NAO. In the AGCM_EML (Fig. 5, left panels), the response in October still exhibits a wave train pattern, but the re-

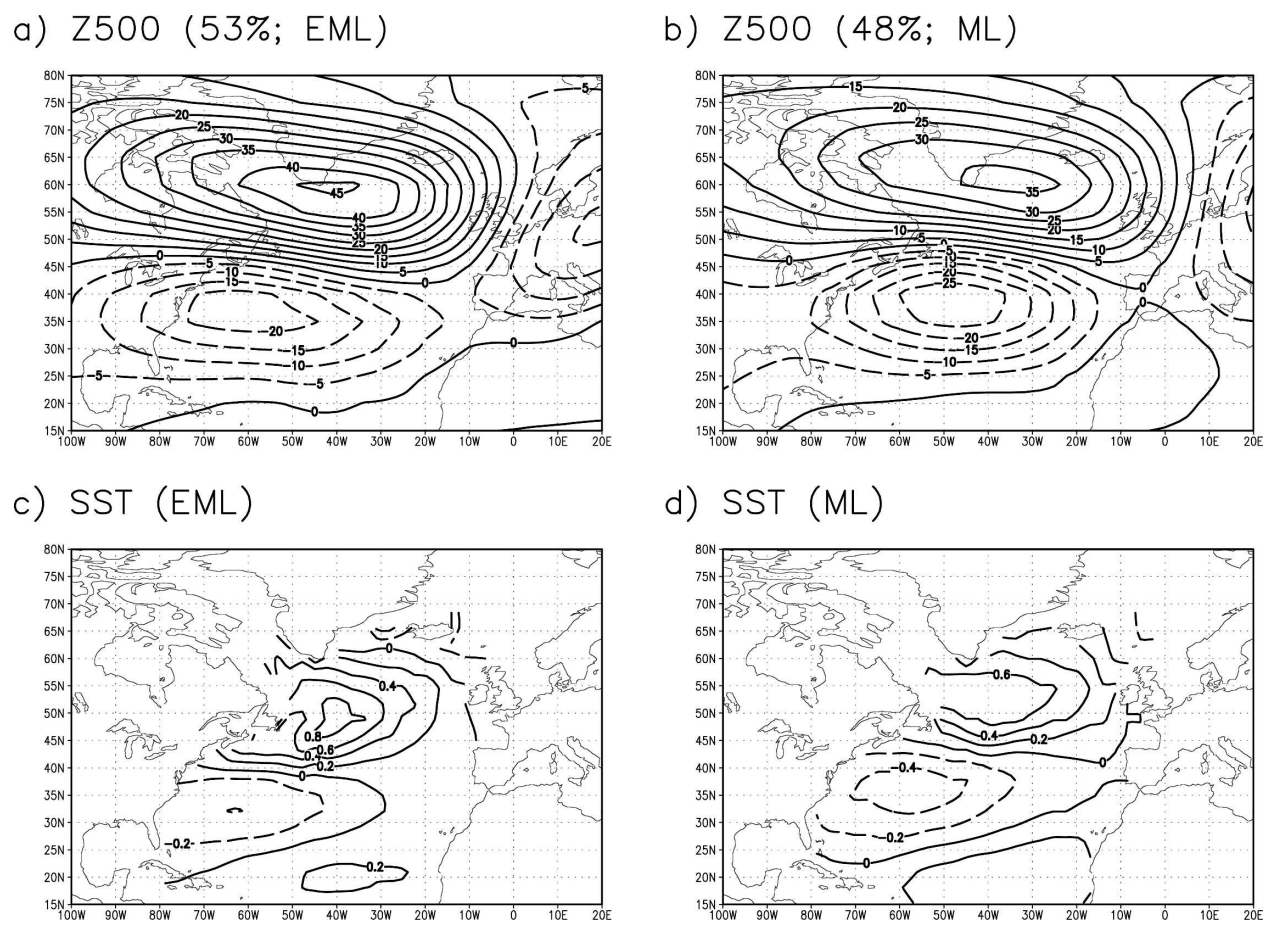

FIG. 3. Heterogeneous Z500 and homogeneous SST covariance maps for the first MCA mode in NDJ in (a), (c) the AGCM_EML control runs and (b), (d) the AGCM_ML control runs. The contour interval is 5 m in (a) and (b), and 0.2 K in (c) and (d). The percentage of the squared covariance explained by the mode is given in the brackets.

sponse in NDJ features a NAO-like north–south dipole with a southern trough about twice as strong as in the AGCM_ML. The response in FMA also features a well-defined NAO dipole, similar to that in the AGCM_ML. The presence of Ekman heat transport in the AGCM_EML thus leads to an earlier development of the NAO response. As a result, the NAO response in the AGCM_EML is more consistent with the observed relationship of CF02 in suggesting that a persistent fall tropical anomaly can induce a NAO in NDJ.

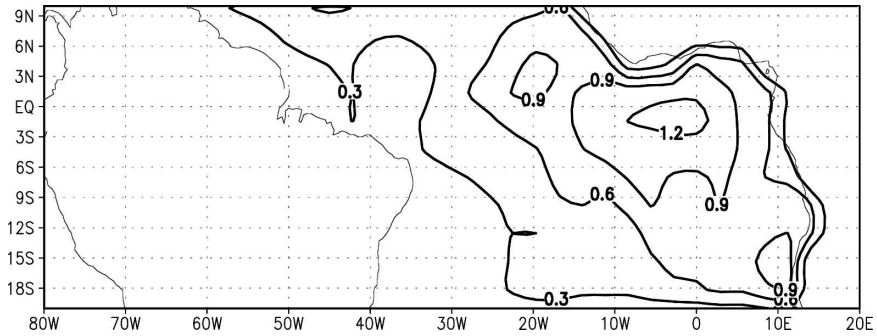

FIG. 4. The tropical SST anomaly used to force the AGCM_EML. The contour interval is 0.3 K.

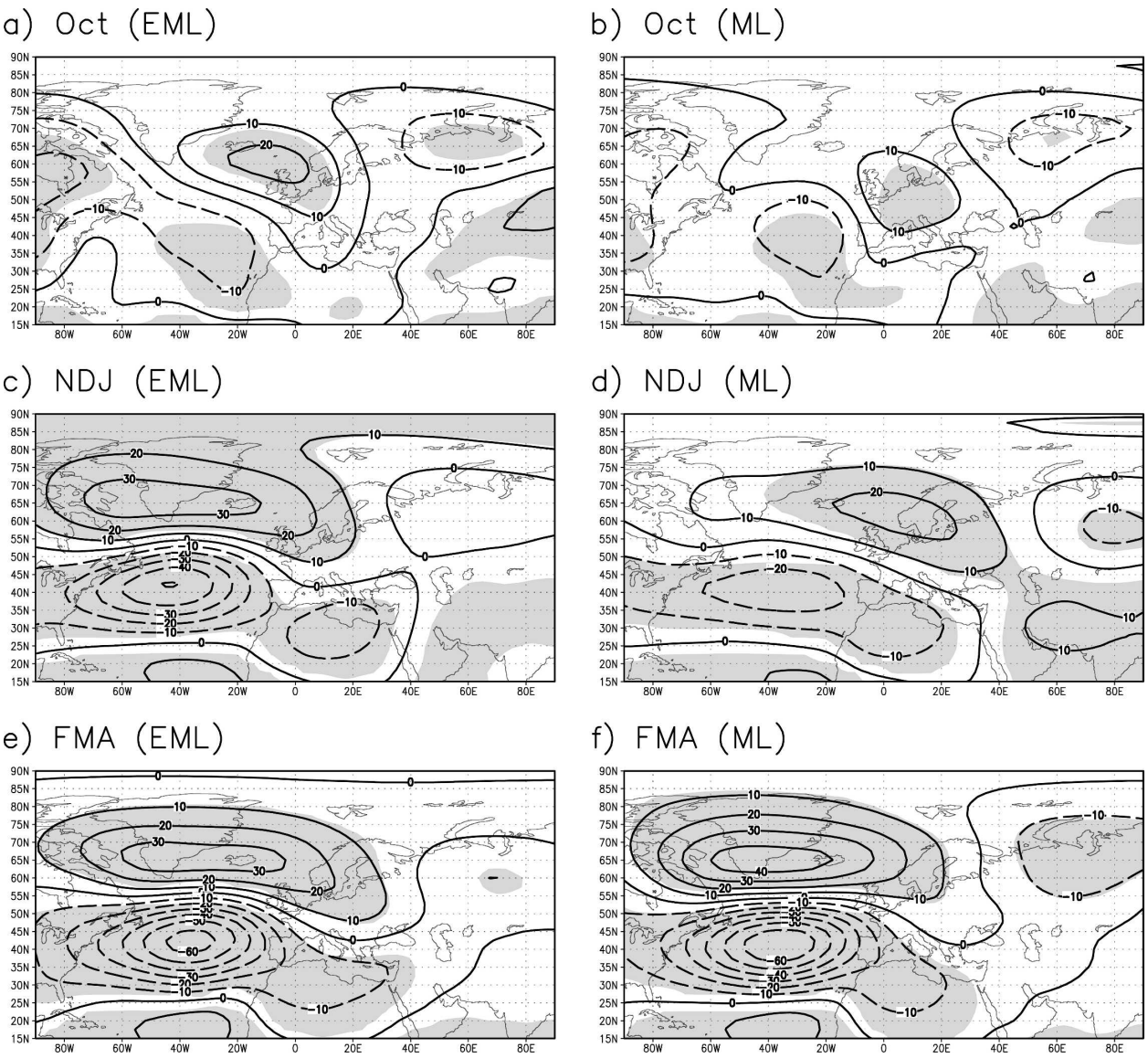

FIG. 5. The Z500 response, as the (P − N) ensemble mean difference, in October, NDJ, and FMA in (a), (c), (e) the AGCM_EML and (b), (d), (f) the AGCM_ML. The contour interval is 10 m. The shading in this and succeeding figures denotes areas where the response is significant at the 95% level, as estimated by a Student's *t* test.

As expected, the corresponding SST response in October in both models is very weak, but a NAH-like pattern, forced by the wave train height response, is still visible (Figs. 6a,b). Consistent with the height response, the SST response in the two models also differs most strongly in NDJ, with a dipolar (or tripolar) anomaly appearing in the AGCM_EML, but a mostly negative anomaly in the AGCM_ML (Figs. 6c,d). The amplitude of the negative center in the AGCM_EML is about twice that in the AGCM_ML, despite the deeper mixed layer in the former. The enhanced coupled response in NDJ in the AGCM_EML suggests that Ekman transport induces a positive extratropical air–sea feedback during these months. In FMA, the SST response in the two models features a similar tripole, but it is stronger in the AGCM_EML (Figs. 6e,f). Given that the SST response is stronger in the AGCM_EML but not the Z500 response, this indicates a saturation of the coupled response in FMA that likely involves a negative air–sea feedback, with partial cancellation between the anomalous heat fluxes and Ekman transports.

To confirm that the differences in the response between the two models, as shown in Figs. 5–6, stem mainly from the differences in the extratropical air–sea

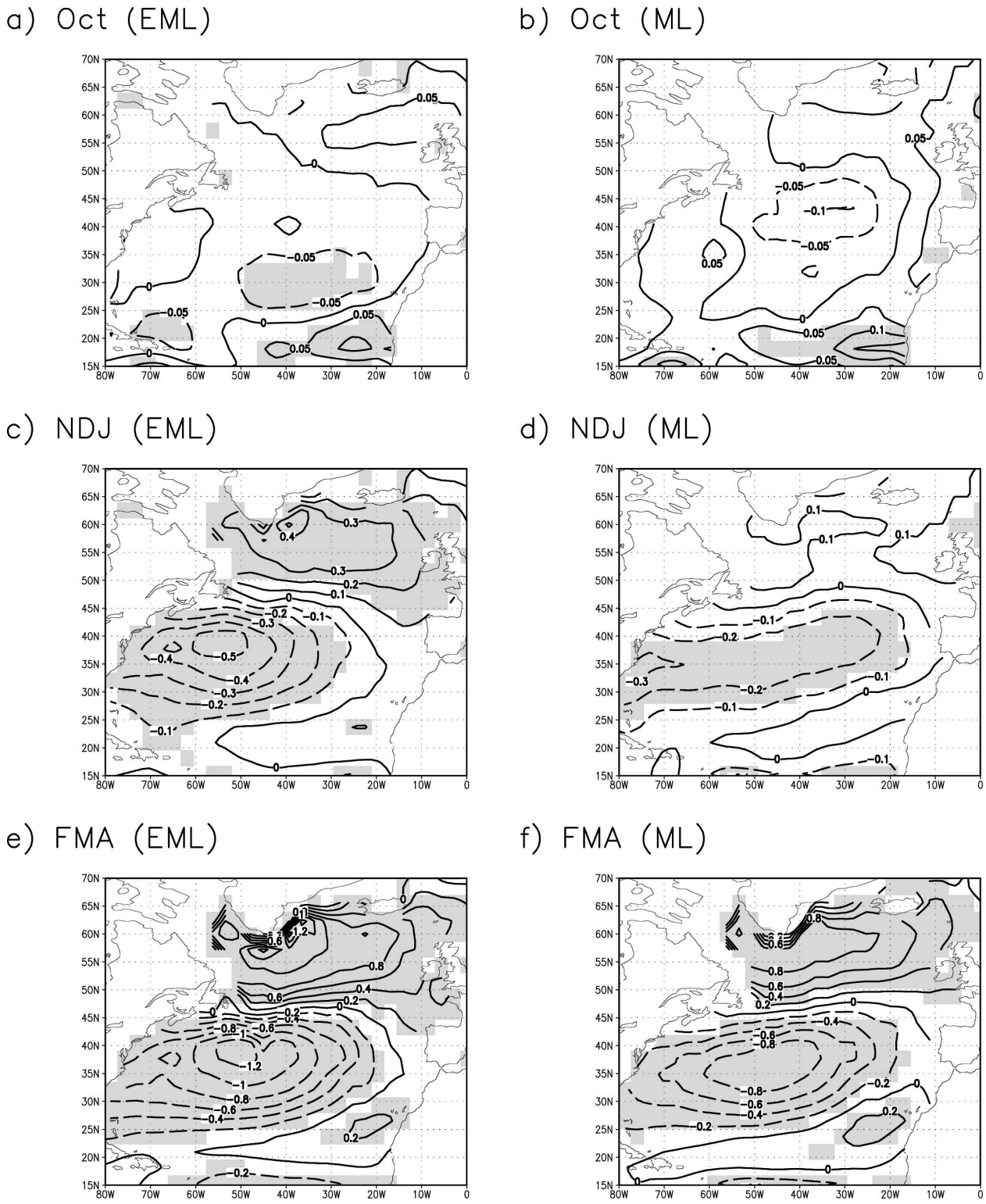

FIG. 6. Same as in Fig. 5 but for the SST response. The contour interval is (a), (b) 0.05; (c), (d) 0.1, and (e), (f) 0.2 K.

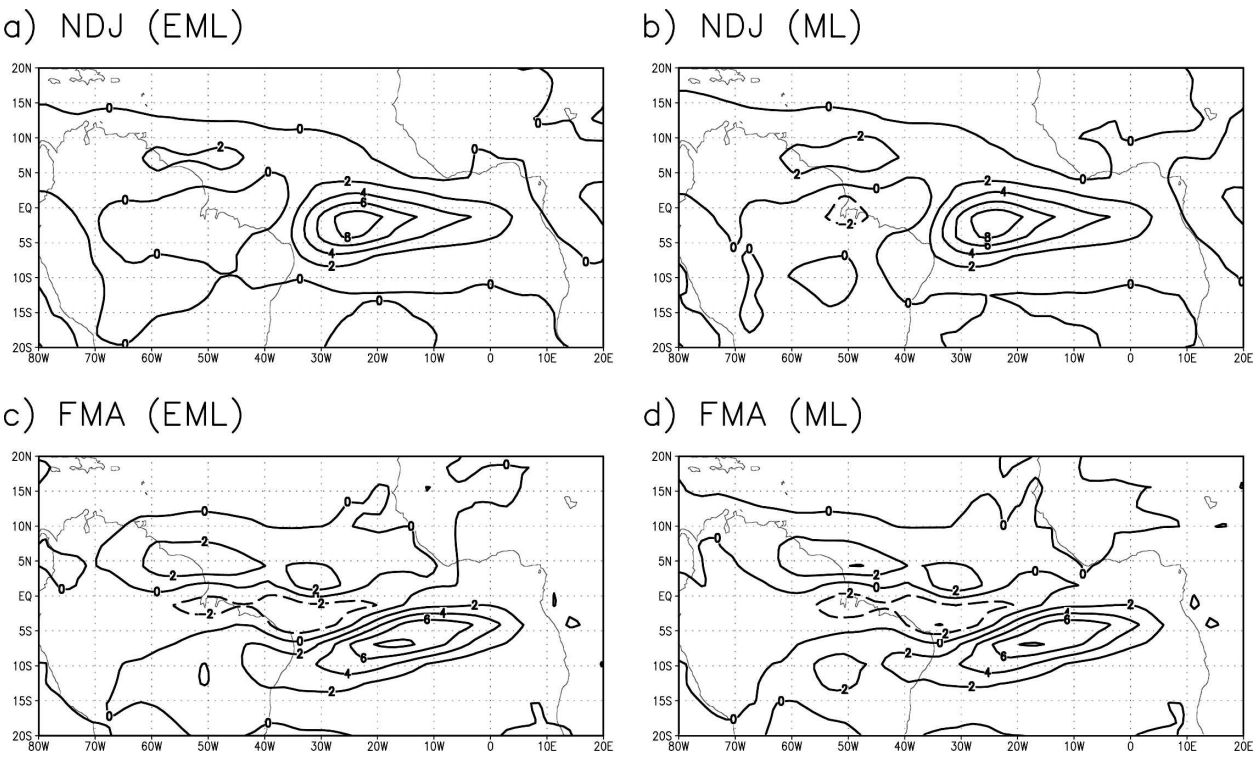

FIG. 7. Same as in Fig. 5 but for the precipitation response in (a), (b) NDJ and (c), (d) FMA. The contour interval is 2 mm day^{-1}.

feedback, the SST-induced response in the tropical precipitation is examined. As shown in Fig. 7, the precipitation response in NDJ in both models features a monopole pattern centered near the equator, and in FMA the main center is shifted to the southeast. The striking similarity in the precipitation response of the two models demonstrates that the inclusion of Ekman transport has little effect on the tropical heating, and the earlier development of the NAO in the AGCM_EML results mainly from the enhanced extratropical SST feedback on the atmosphere. The linear model results of Peng et al. (2005) revealed that, in the absence of extratropical SST and transient eddy feedbacks, the tropical heating invariably induces a wave train–like response, regardless of the details of the heating. Peng et al. (2003) also showed that an extratropical tripolar SST induces a NAO response mainly through an eddy-feedback mechanism, by effectively perturbing the Atlantic storm track. These mechanisms are believed to be similarly at work in producing the tropically forced NAO responses in these coupled models.

The SST response in the AGCM_EML is determined by the anomalous surface heat flux and Ekman advection and in the AGCM_ML by only the anomalous surface heat flux. As shown in Figs. 8b–d, the response, in the surface heat flux, induced by the tropical SST anomaly in the AGCM_ML is weaker in NDJ and stronger in FMA, corresponding to the growth with time of the coupled response. In the AGCM_EML, however, the response in the total heat transport (including the surface heat flux and the Ekman advection) is much stronger in NDJ than in FMA (Figs. 8a,c).[1] This indicates a faster approach of the coupled response in the AGCM_EML to its equilibrium. Comparing the response in NDJ in the two models (Figs. 8a,b) reveals that, due to the effects of Ekman transport, the response in the total heat transport in the AGCM_EML is more than 3 times as strong as the response in the surface heat flux in the AGCM_ML. In FMA, the strength of the response in the two models (Figs. 8c,d) is comparable. Due to the difference in the MLD in the two models, the accumulated change in the SST response over NDJ is about twice as strong in the AGCM_EML as that in the AGCM_ML (~0.8 versus

[1] The anomalous Ekman advection shown in Figs. 8a,c is calculated using the monthly ensemble mean wind stress and SST, as the daily wind stress data were accidentally lost. To verify that the daily deviations from the monthly ensemble mean contribute little to the mean response, we examined the change of the SST anomaly over NDJ and over FMA using the daily ensemble mean SST data, and found that it is indeed consistent with the response in the total heat transport shown in Figs. 8a,c.

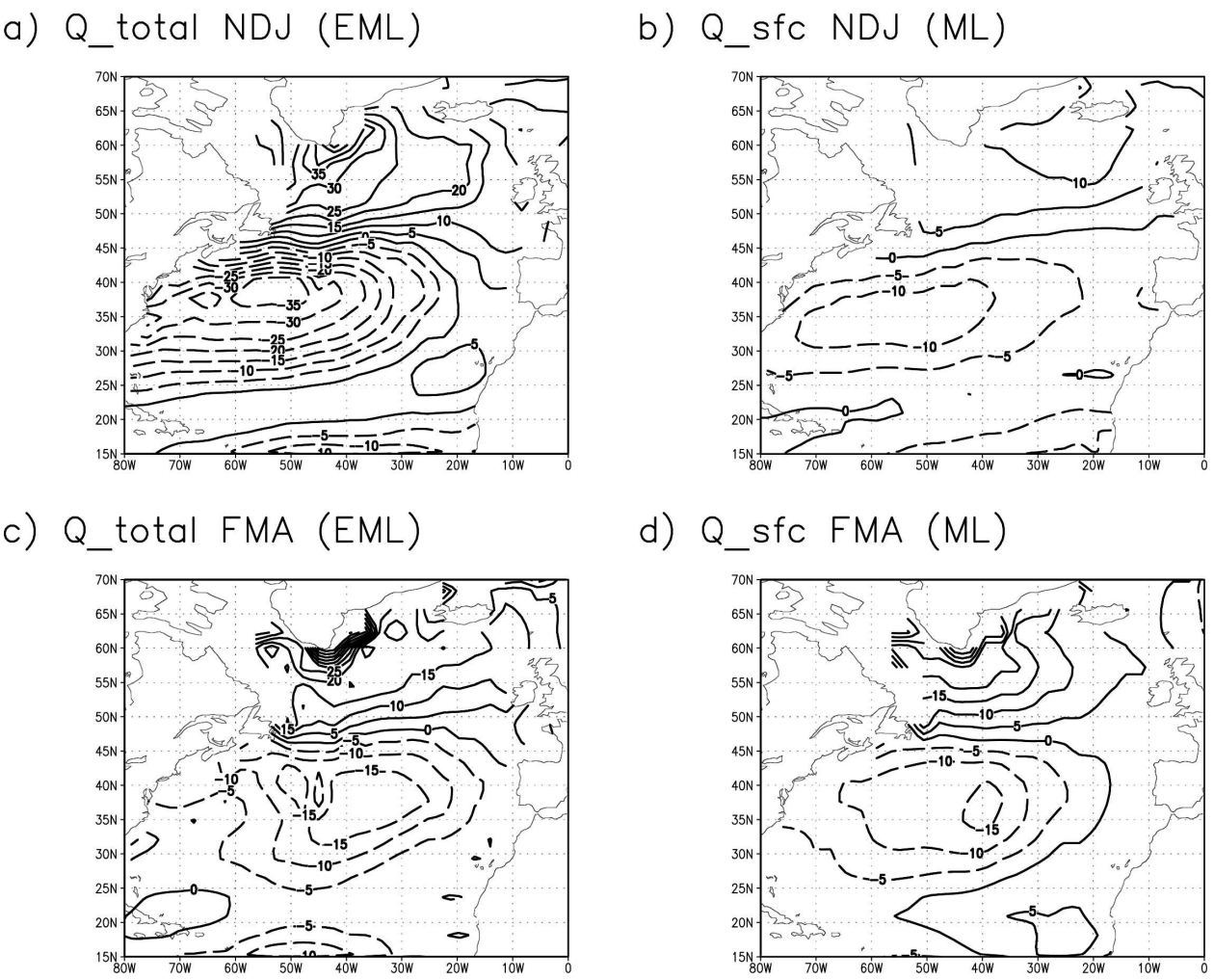

FIG. 8. Same as in Fig. 5 but for the response in NDJ and FMA in (a), (c) the total heat transport in the AGCM_EML and (b), (d) the surface heat flux in the AGCM_ML. The contour interval is 5 W m^{-2}.

0.4 K), in proportion to the anomalous total heat transport and surface heat flux shown in Figs. 8a,b. The corresponding change in the SST response over FMA is weaker in the AGCM_EML than that in the AGCM_ML (~0.4 versus 0.6 K).

To further elucidate the role of Ekman transport in inducing the enhanced coupled response in NDJ, the response in the total heat transport in the AGCM_EML is decomposed into three components: the response in the surface heat flux and in the two Ekman advection terms [Eq. (2.1)]. As shown in Figs. 9a,b, the response in the surface heat flux in the AGCM_EML is much stronger in NDJ than that in FMA, and their patterns are noticeably different. The anomalous heat transport due to the advection of the mean temperature by the anomalous Ekman currents (Figs. 9c,d) exhibits a dipole in the western Atlantic, similar in NDJ and FMA. This component of the anomalous Ekman transport contributes significantly to the SST response; its amplitude is on the same order as that of the anomalous surface heat flux. The anomalous heat transport due to the advection of the anomalous temperature by the mean Ekman currents (Figs. 9e,f) is much weaker and plays a minor role in the heat budget.

Comparing Figs. 9a,c reveals that, in NDJ, the dipolar anomalous Ekman transport tends to reinforce the response in the surface heat flux. The combined effect of these two processes results in a faster growth in the SST response (Fig. 6c) than from the heat flux alone. The feedback of the dipolar SST anomaly on the atmosphere, in turn, accelerates the development of the NAO-like Z500 response (Fig. 5c) in NDJ in the AGCM_EML, compared with the AGCM_ML. These processes that enhance the tropically forced NAO re-

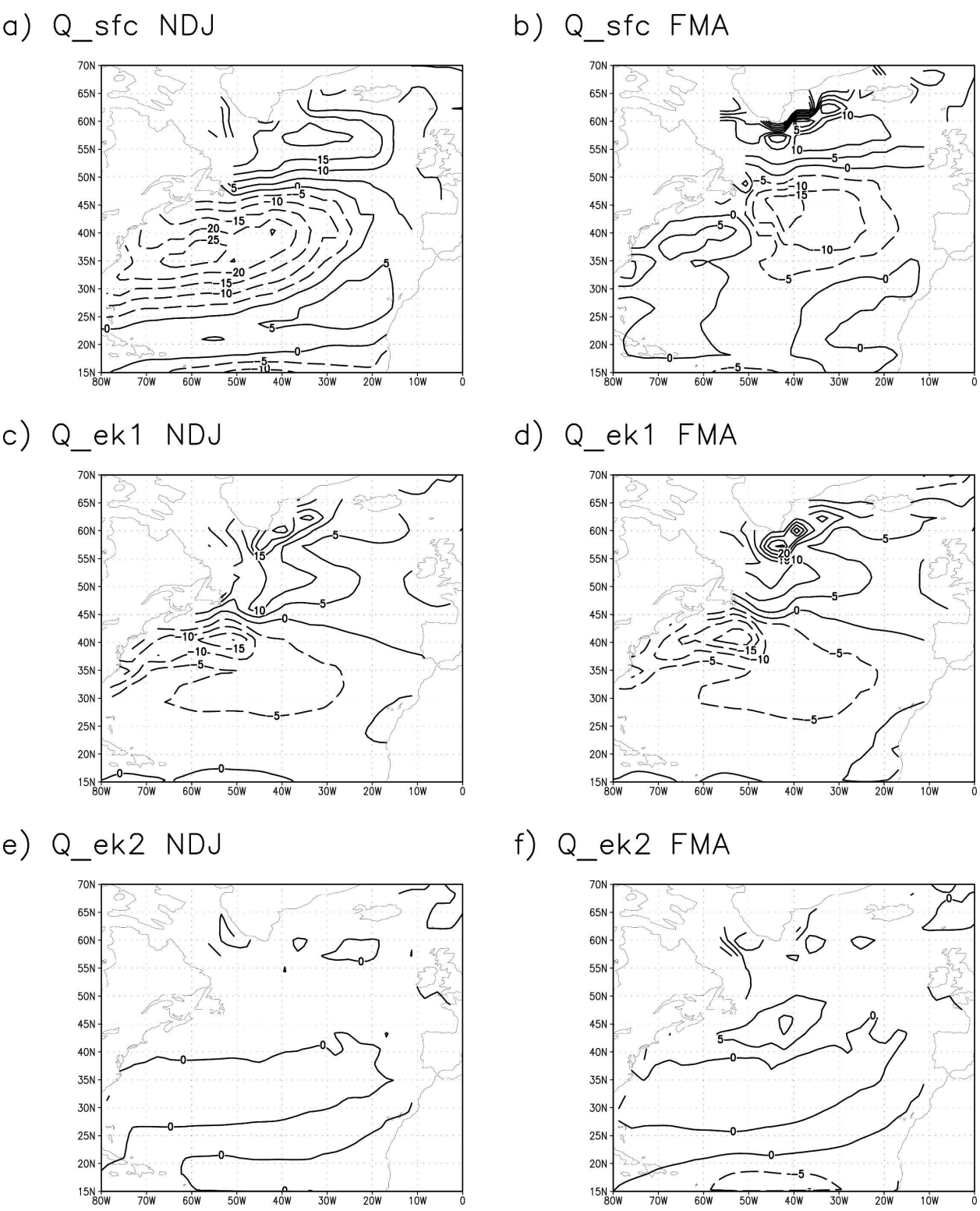

FIG. 9. Same as in Fig. 8 but for the AGCM_EML response in (a), (b) the surface heat flux; (c), (d) the advection of the climatological temperature by the anomalous Ekman current; and (e), (f) the advection of the anomalous temperature by the climatological Ekman current. The contour interval is 5 W m^{-2}.

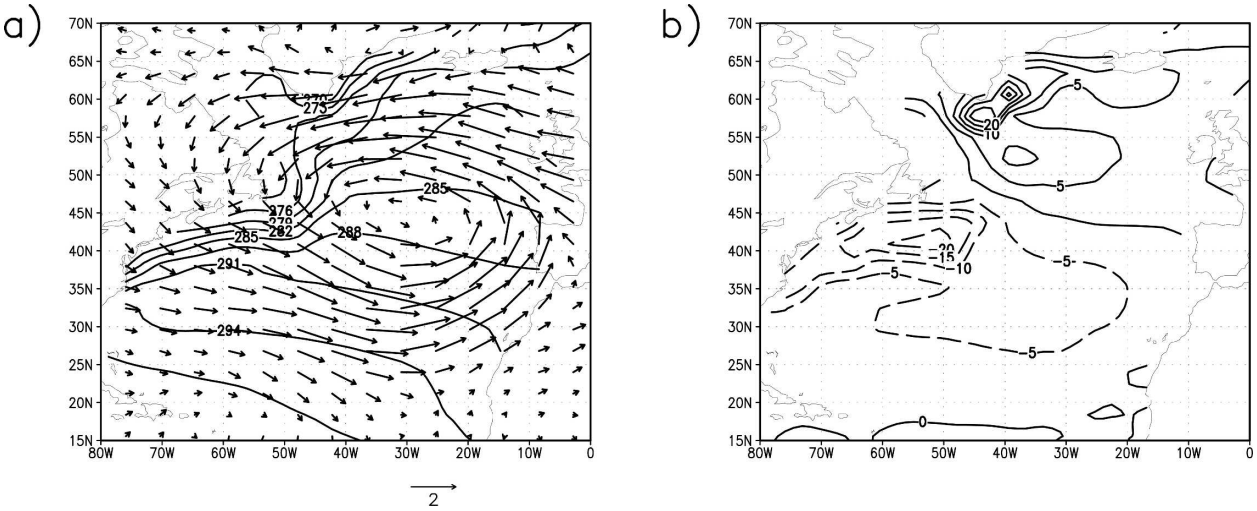

FIG. 10. (a) The AGCM_EML response in the wind at 10 m (vectors; m s^{-1}) in FMA, and the corresponding SST climatology (contours). (b) The response in the advection of the climatological temperature by the anomalous meridional Ekman current in FMA. The contour interval is (a) 3 K and (b) 5 W m^{-2}.

sponse in NDJ are likely responsible for the enhanced coupled NAO–SST tripole variability in NDJ in the AGCM_EML control runs (Fig. 3). In FMA, the anomalous Ekman transport (Fig. 9d) remains similar to that in NDJ, except stronger, but the response in the surface heat flux (Fig. 9b) is much weakened as the anomalous air–sea temperature difference is reduced. In fact, south of Newfoundland along the path of Gulf Stream where the anomalous negative Ekman transport is strongest, the sign of the anomalous heat flux is now reversed and counteracts the anomalous Ekman transport. This adjustment in the surface heat flux is likely crucial in determining how the coupled response equilibrates. A similar sign reversal in the anomalous heat flux is also associated with the equilibrium response in the AGCM_ML, but it occurs later in the season.

The dipolar anomalous Ekman transport depicted in Figs. 9c,d is dominated by its meridional component, the advection of the mean temperature by the anomalous meridional Ekman current. Since the anomalous surface wind is similar in NDJ and FMA, the wind anomaly at 10 m averaged over FMA is shown in Fig. 10a, along with the corresponding SST climatology. The anomalous wind in the North Atlantic is dominated by a cyclonic circulation, with westerlies south of 45°N and easterlies to the north. Since Ekman currents are directed to the right of the wind stress, their meridional components generate a dipolar anomalous transport, with cold advection south of 45°N and warm advection to the north as depicted in Fig. 10b.

The seasonal responses shown in Figs. 5–9 demonstrate that, due to reinforcement between the anomalous Ekman transport and surface heat flux, the coupled NAO–SST tripole response develops more rapidly in the AGCM_EML than in the AGCM_ML. To further illustrate the difference in the monthly evolution of the Z500 and the SST response in the two models, the spatial rms of the Z500 response over the area of 25°–85°N and 80°W–20°E (as a measure of the strength of the response) is plotted in Fig. 11a, along with the rms of the SST response (20°–60°N and 70°–20°W) in Fig. 11b. During the initial months, the anomalous SST grows faster in the AGCM_EML (solid line) than that in the AGCM_ML (dashed line) as expected. Correspondingly, the amplitude of the Z500 response in the AGCM_EML also grows faster and reaches its maximum one to two months earlier, in January, in comparison with that in the AGCM_ML. A weakening of the Z500 response after its maximum appears to occur in both models, but more quickly in the AGCM_EML (i.e., February versus April). This weakening is likely related to the weakening (and even the sign reversal in some areas) in the anomalous surface heat flux, as indicated in the reduced growth rate in the SST response after January in the AGCM_EML and after March in the AGCM_ML. The strength of the mean equilibrium Z500 response (i.e., the average over January–April for the AGCM_EML and over February–April for the AGCM_ML) in the two models is closely comparable. Hence, the inclusion of Ekman transport primarily accelerates the development of the coupled response.

Because of this acceleration, the response generated in the two models, for a given month, can differ significantly, as shown in Fig. 12. In January, the Z500 re-

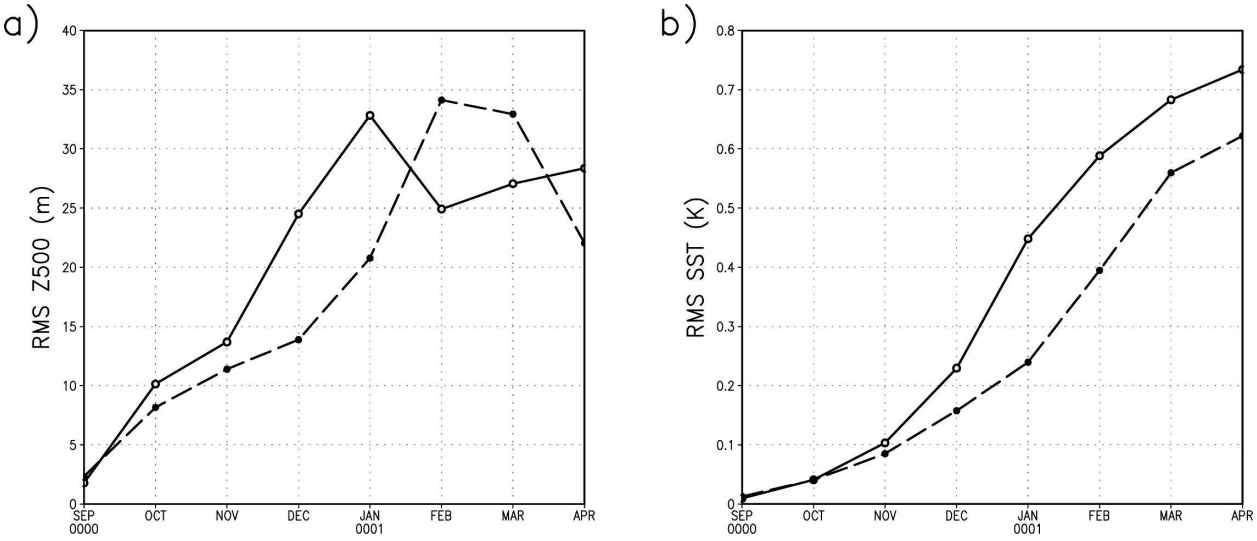

FIG. 11. Spatial rms of (a) the Z500 response (25°–85°N and 80°W–20°E) and (b) the SST response (20°–60°N and 70°–20°W) during the 8-month integration period from September to April in the AGCM_EML (solid line) and in the AGCM_ML (dashed line).

sponse in the AGCM_EML (Fig. 12a) reaches its maximum with a well-defined north–south NAO dipole of about 50 and −70 m in the two centers. The corresponding Z500 response in the AGCM_ML (Fig. 12b) is much weaker (40 and −40 m) with its positive center shifted to the east. The pattern of the SST response in January in the two models is similar to that shown in Figs. 6c,d, but the amplitude is about twice as strong. For comparison, we also show in Fig. 12c the Z500 response in January in the uncoupled AGCM. The AGCM response is dominated by a trough in the North Atlantic with a wave train downstream. The marked

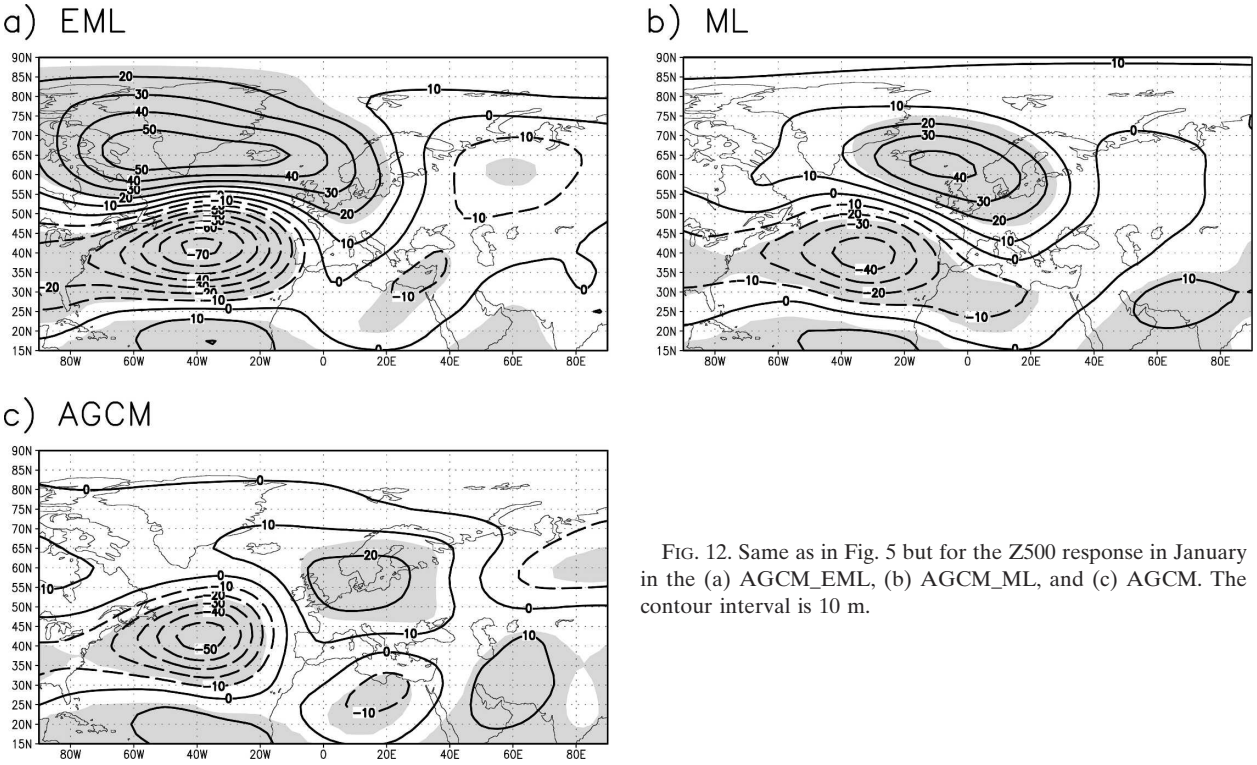

FIG. 12. Same as in Fig. 5 but for the Z500 response in January in the (a) AGCM_EML, (b) AGCM_ML, and (c) AGCM. The contour interval is 10 m.

differences in these responses suggest that extratropical SST feedback plays a significant role in the development of the NAO response to tropical forcing.

4. Summary and discussion

The results of the coupled AGCM_ML experiments of Peng et al. (2005) demonstrate that a persistent tropical Atlantic SST anomaly induces a coupled NAO–SST tripole response in late winter (FMA), which is 1–2 months later than that indicated by the observations (CF02). To determine if this discrepancy in the seasonality of the simulated response is due, in part, to the lack of Ekman transports in the slab ocean model, a new coupled model, AGCM_EML, is developed with Ekman heat transport included. Large ensembles of AGCM_EML experiments are conducted to determine the effects of Ekman transport on the development of the coupled response to the same tropical SST anomaly as was used by Peng et al. (2005).

The model results reveal that the inclusion of Ekman transport indeed leads to an earlier development of the coupled NAO–SST tripole response in the AGCM_EML than in the AGCM_ML. Due to the reinforcement between the anomalous Ekman transport and surface heat flux, the tropical SST anomaly induces an extratropical SST response in NDJ in the AGCM_EML twice as strong as in the AGCM_ML, even though a deeper mixed layer is used in the AGCM_EML. The feedback of the SST response on the atmosphere, in turn, produces the NAO response early in the winter. These results suggest that a persistent tropical SST anomaly in the fall can induce a coupled NAO–SST tripole response in NDJ, as indicated by the observed lagged relationship shown by CF02. Consistent with the forced response, the inclusion of Ekman transport also leads to enhanced coupled NAO–SST tripole variability in NDJ in the AGCM_EML control runs.

In FMA, the anomalous air–sea temperature difference is reduced due to the growth of the extratropical SST anomaly. The anomalous surface heat flux weakens, and even reverses its sign in the Gulf Stream region to oppose the anomalous Ekman transport. This sign reversal is suspected to be instrumental in allowing the coupled response to equilibrate, though the detailed process remains to be fully established in future studies. The equilibrium NAO responses averaged over FMA in the two models are similar in their patterns and amplitudes, but the equilibrium is reached sooner in the AGCM_EML. The maximum NAO response is reached in January in the AGCM_EML, one month earlier than in the AGCM_ML. Thus, the inclusion of Ekman transport in the AGCM_EML acts primarily to cause a seasonal shift in the evolution of the coupled response to the tropical forcing.

Considering that, in nature, tropical SST anomalies rarely persist for 8 months, as in the present model experiments, the faster development of the NAO response in the AGCM_EML makes it more likely than was indicated by the results of Peng et al. (2005) that tropical SST anomalies influence the NAO within a single season. The present results further strengthen the evidence supporting a significant role for interactions with the extratropical ocean in developing the NAO response. It is likely that Ekman transport also affects other remotely and locally forced coupled variability. How strongly a coupled anomaly may be influenced by Ekman transport likely depends on the relationship between the associated anomalous Ekman transport and the surface heat flux, as has been illustrated in this study. Possibly, the dominant structures of coupled low-frequency variability observed in nature result from the combined effects of several mutually reinforcing processes, including Ekman transport. A systematic study is required to elucidate such processes and how they operate in relation to different patterns of coupled variability.

It is noted that the NAH SST anomaly simulated in the AGCM_ML in Peng et al. (2005), and also hinted here in the AGCM_EML, differs to some extent from the JAS NAH pattern highlighted in CF02. We believe that these differences are mainly due to the difference in the season, as the model simulations in our studies start a few months later, in September; a more similar NAH anomaly will likely be produced if the simulations start earlier. One should keep in mind, however, that even when the observed JAS NAH anomaly is used to directly force the AGCM, it fails to induce a NAO response, as demonstrated in Peng et al. (2005; see also Rodwell et al. 2004). These results indicate it is unlikely that local air–sea interactions drive the observed NAH SST–NAO lagged relationship. We do not expect the nature of the NAH anomaly–induced response to change significantly even in coupled models. Comparing the SST tripole–induced response in the AGCM of Peng et al. (2003) and that in the fully coupled model of Wu and Liu (2005) suggests that the response is qualitatively similar in the uncoupled and coupled models. Nevertheless, these could be verified with further systematic experiments.

Acknowledgments. We acknowledge the support of Drs. Martin P. Hoerling and Klaus M. Weickmann for this project. Helpful discussions with Dr. Amy Solomon on the formulation of the model are appreciated. We also thank the two reviewers for their thoughtful com-

ments on the manuscript. This research is supported in part by funding from the NOAA's CLIVAR Atlantic Program.

REFERENCES

Alexander, M. A., C. Deser, and M. S. Timlin, 1999: The re-emergence of SST anomalies in the North Pacific Ocean. *J. Climate,* **12,** 2419–2431.

——, I. Blade, M. Newman, J. R. Lanzante, N.-C. Lau, and J. D. Scott, 2002: The atmospheric bridge: The influence of ENSO teleconnections on air–sea interaction over the global oceans. *J. Climate,* **15,** 2205–2231.

Cassou, C., C. Deser, L. Terray, J. W. Hurrell, and M. Drévillon, 2004: Summer sea surface temperature conditions in the North Atlantic and their impact upon the atmospheric circulation in early winter. *J. Climate,* **17,** 3349–3363.

Czaja, A., and C. Frankignoul, 2002: Observed impact of Atlantic SST anomalies on the North Atlantic Oscillation. *J. Climate,* **15,** 606–623.

Deser, C., and M. L. Blackmon, 1993: Surface climate variations over the North Atlantic Ocean during winter: 1900–1993. *J. Climate,* **6,** 1743–1753.

Drevillon, M., C. Cassou, and L. Terray, 2003: Model study of the North Atlantic region atmospheric response to autumn tropical Atlantic sea-surface-temperature anomalies. *Quart. J. Roy. Meteor. Soc.,* **129,** 2591–2611.

Ferreira, D., and C. Frankignoul, 2005: The transient atmospheric response to midlatitude SST anomalies. *J. Climate,* **18,** 1049–1067.

Frankignoul, C., 1985: Sea surface temperature anomalies, planetary waves, and air-sea feedback in the midlatitudes. *Rev. Geophys.,* **23,** 357–390.

——, and E. Kestenare, 2005: Observed Atlantic SST anomaly impact on the NAO: An update. *J. Climate,* **18,** 4089–4094.

Haarsma, R. J., E. J. D. Campos, W. Hazeleger, C. Severijns, A. R. Piola, and F. Molteni, 2005: Dominant modes of variability in the South Atlantic: A study with a hierarchy of ocean–atmosphere models. *J. Climate,* **18,** 1719–1735.

Kushnir, Y., 1994: Interdecadal variations in North Atlantic sea surface temperature and associated atmospheric conditions. *J. Climate,* **7,** 142–157.

Lau, N.-C., and M. J. Nath, 1996: The role of the "atmospheric bridge" in linking tropical Pacific ENSO events to extratropical SST anomalies. *J. Climate,* **9,** 2036–2057.

Marshall, J., and Coauthors, 2001: North Atlantic climate variability: Phenomena, impacts, and mechanisms. *Int. J. Climatol.,* **21,** 1863–1898.

Peng, S., W. A. Robinson, and S. Li, 2002: North Atlantic SST forcing of the NAO and relationships with intrinsic hemispheric variability. *Geophys. Res. Lett.,* **29,** 1276, doi:10.1029/2001GL014043.

——, ——, and ——, 2003: Mechanisms for the NAO responses to the North Atlantic SST tripole. *J. Climate,* **16,** 1987–2004.

——, ——, ——, and M. P. Hoerling, 2005: Tropical Atlantic SST forcing of coupled North Atlantic seasonal responses. *J. Climate,* **18,** 480–496.

Rodwell, M. J., D. P. Rowell, and C. K. Folland, 1999: Oceanic forcing of the wintertime North Atlantic Oscillation and European climate. *Nature,* **398,** 320–323.

——, M. Drevillon, C. Frankignoul, J. W. Hurrell, H. Pohlmann, M. Stendel, and R. T. Sutton, 2004: North Atlantic forcing of climate and its uncertainty from a multimodel experiment. *Quart. J. Roy. Meteor. Soc.,* **130,** 2013–2032.

Seager, R., Y. Kushnir, M. Visbeck, N. Naik, J. Miller, G. Krahmann, and H. Cullen, 2000: Causes of Atlantic Ocean climate variability between 1958 and 1998. *J. Climate,* **13,** 2845–2862.

——, ——, N. H. Naik, M. A. Cane, and J. Miller, 2001: Wind-driven shifts in the latitude of the Kuroshio–Oyashio extension and generation of SST anomalies on decadal timescales. *J. Climate,* **14,** 4249–4265.

Sutton, R. T., W. A. Norton, and S. P. Jewson, 2001: The North Atlantic Oscillation—What role for the ocean? *Atmos. Sci. Lett.,* **1,** 89–100.

Watanabe, M., and M. Kimoto, 2000: Atmosphere-ocean thermal coupling in the North Atlantic: A positive feedback. *Quart. J. Roy. Meteor. Soc.,* **126,** 3343–3369.

Wu, L., and Z. Liu, 2005: North Atlantic decadal variability: Air–sea coupling, oceanic memory, and potential Northern Hemisphere resonance. *J. Climate,* **18,** 331–349.